has been suggested[7] for the correlation function $\langle\vec{\sigma}_1\cdot\vec{\sigma}_j\rangle$ in the Heisenberg model. Our susceptibility, however, diverges with a $(T-T_c)^{-1}$ law which differs from the nonentire power law proposed[2] for the Heisenberg model.

It may be worth emphasizing again that, in the present model, T_c is not a thermodynamical singularity; moreover, T_c depends on that wave number $\vec{K}$ which has been considered.

It is possible that the above considerations might serve as a guide for obtaining further results on the two-dimensional Heisenberg model, and perhaps on the hard-disc system.[8]

*Laboratoire associé au Centre National de la Recherche Scientifique.

[1]N. D. Mermin and H. Wagner, Phys. Rev. Letters 17, 1133 (1966).

[2]H. E. Stanley and T. A. Kaplan, Phys. Rev. Letters 17, 913 (1966).

[3]We assume, only for the sake of simpler notations, that the phonon frequency does not depend on its polarization.

[4]J. Yvon, Nuovo Cimento Suppl. 6, 187 (1949).

[5]The limit $N\to\infty$ can be taken at the present stage. One could, however, get incorrect results by taking that limit too early, for instance in (8).

[6]For a one-dimensional lattice, the analog of (8) increases linearly with R, and $\chi_{\vec{K}}$ is finite at any temperature.

[7]F. J. Dyson, private communication to H. E. Stanley and T. A. Kaplan.

[8]B. J. Alder and T. E. Wainwright, Phys. Rev. 127, 359 (1962).

ABSOLUTE MEASUREMENT OF STRUCTURE FACTORS WITH HIGH PRECISION

N. Kato and S. Tanemura
Department of Applied Physics, Faculty of Engineering, Nagoya University, Nagoya, Japan
(Received 15 May 1967)

Recently, Hattori et al. have measured the structure factors of Si single crystals on the absolute scale with an accuracy of about 1%.[1,2] The method is entirely different from the conventional one based on x-ray intensity measurements. The new method is based on the spacing measurement of the Pendellösung fringes[3] due to the interference of doubly refracted x rays under the condition of the Bragg reflection. The results are free from extinction effects and less ambiguous in applying the theoretical formula connecting the structure factor $|F_g|$ with the observable quantities.

The spacing $\Lambda_g{}^c$ of the Pendellösung fringes along the net plane is given by[1,2,4]

$$\Lambda_g{}^c=\frac{\pi v}{\lambda\cos\theta_B}\left(\frac{mc^2}{e^2}\right)|F_g|^{-1}, \tag{1}$$

including the effect of x-ray polarization, where λ is the wavelength, θ_B is the Bragg angle, v is the volume of unit cell, and e, m, and c are the physical constants having usual meanings. The observable spacing Λ_g is connected with this spacing $\Lambda_g{}^c$ through a geometrical factor Φ_g:

$$\Lambda_g=\Lambda_g{}^c\Phi_g. \tag{2}$$

If a perfect wedge crystal of wedge angle φ is used and either the entrance surface or the exit surface of the crystal is perpendicular to the plane determined by the incident beam and the Bragg-reflected beam, the factor Φ_g turns out to be $\cot\varphi$.

We confirmed through internal check that Λ_g itself could be determined with an accuracy of about 0.1% under suitable experimental conditions, particularly in low-order reflections. A difficulty, however, for obtaining $|F_g|$ accurately arises in determining the wedge angle φ with sufficient accuracy. Moreover, it is rather difficult to prepare an ideally perfect wedge of the crystal. For this reason, in the previous work, the accuracy of the structure factor was not better than about 1%.

Here, it is shown that the geometrical factor Φ_g can be eliminated by combining the experiment of Pendellösung fringes with that of thickness fringes in x-ray interferometry which has been recently demonstrated by Bonse and Hart.[5] The principle of the present interferometer is illustrated in Fig. 1. The incident beam satisfies the Bragg condition simultaneously at the interferometer crystals S, M, and A. Contrary to that of Bonse and Hart, an extremely narrow beam (20~100 μ) was used

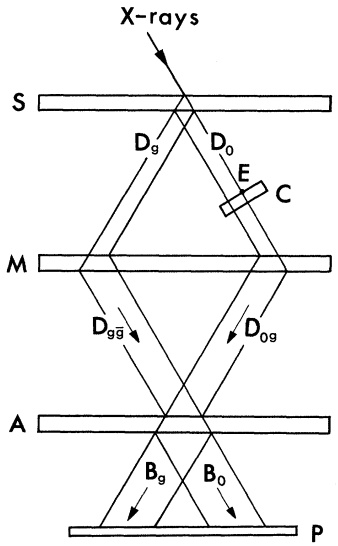

FIG. 1. The relations among the interferometer crystals (S, M, and A) and x-ray beams. P is the photographic plate.

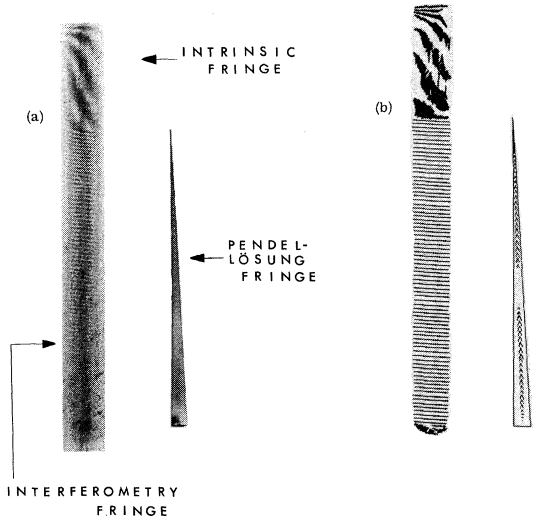

FIG. 2. Photograph (a) and schematic illustration (b) of the three kinds of fringes. The tip of the Pendellösung fringes corresponds to the boundary between the intrinsic fringes and the interferometry fringes. If the specimen crystal is absent, the intrinsic fringes cover the region of the interferometry fringes.

in order to specify the optical path inside the crystal. In addition, Ag $K\alpha_1$ radiation was used in order to eliminate absorption effects in the speciment (C). Since thick crystal slices (~2.4 mm) were used for the interferometer, the Borrmann effect required was large enough in each slice. The interference takes place between two x-ray waves divided by the splitter crystal S. The fringes appear in the beams B_0 and B_g, in which the divided waves are overlapped. By the principle of the present interferometer,[6,7] we can easily see that the fringe spacing Λ_0 in the middle of the beam B_0 or B_g is given by

$$\Lambda_0 = \Lambda_0{}^c \Phi_0, \tag{3}$$

$$\Lambda_0{}^c = 2\frac{\pi v}{\lambda}\left(\frac{mc^2}{e^2}\right)\frac{1}{F_0}. \tag{4}$$

Here, $\Lambda_0{}^c$ is the spacing of the virtual fringes which might be observed inside the crystal, if the x-ray wave D_g were superposed on the corresponding wave D_0 in Fig. 1. The factor Φ_0 is again a geometrical factor which connects the virtual fringe spacing with the observable fringe spacing. Thus, we can see that, if the Pendellösung fringes and the interferometry fringes are produced for the same optical path in the crystal, the structure factor $|F_g|$ can be given on the scale of F_0 without knowing the geometrical factor $\Phi_0 = \Phi_g$; i.e.,

$$|F_g|/F_0 = (\Lambda_0/\Lambda_g)/2\cos\theta_B. \tag{5}$$

Since F_0 is the number of electrons in the unit cell, $|F_g|$ is determined on the truly absolute scale.

The Pendellösung fringes and the interferometry fringes are shown in Fig. 2. The x rays which give the minimum fringe spacing of the recorded Pendellösung fringes propagate practically along the concerned net plane passing through the entrance point E in Fig. 1. The interferometry fringes of the middle of B_0 or B_g are produced by the x rays in the middle of the beam D_0. We could, therefore, realize the condition $\Phi_0 = \Phi_g$ in taking the interferometry fringes by rotating the specimen crystal (C) by the Bragg angle θ_B and by traversing the crystal by the half-width of the x-ray beam D_0, after taking the Pendellösung fringes with the same incident beam.

Some of the results on Si single crystals are listed in Table I. For actual cases, we must take several precautions in getting the geometrical conditions to be satisfied for the x-ray beam, the interferometer crystal, the specimen, and the photographic plate. All of the conceivable errors due to misadjustments can be corrected by geometrical considerations.

Table. I. The structure factors of Si.

hkl	$\lvert F_g \rvert$
111	63.2_9, 63.4_3
220	67.2_8

Roughly speaking, the required accuracy in the geometrical setting must be to about 1° for attaining the accuracy of 0.1% in $|F_g|$. Another important correction should be performed properly for the lack of ideally perfect interferometer. In fact, several intrinsic fringes were recorded in the beams B_0 and B_g even when the specimen crystal was absent. The results mentioned above were obtained tentatively on the assumption that the intrinsic fringes were equally spaced. In principle, however, we can eliminate the error due to this assumption without difficulty.

The details of the principle, the apparatus used, and the refined results will be presented shortly elsewhere. The results obtained by the present method may give the knowledge on accurate charge distribution in crystals and make it possible to criticize the conventional method of determining the structure factors.

[1]H. Hattori, H. Kuriyama, T. Katagawa, and N. Kato, J. Phys. Soc. Japan 20, 988 (1965).
[2]H. Hattori, H. Kuriyama, and N. Kato, J. Phys. Soc. Japan 20, 1047 (1965).
[3]N. Kato and A. R. Lang, Acta Cryst. 12, 787 (1959).
[4]N. Kato, Z. Naturforsch. 15a, 369 (1960); Acta Cryst. 14, 526, 627 (1961).
[5]U. Bonse and M. Hart, Appl. Phys. Letters 6, 155 (1965); 7, 99 (1965).
[6]U. Bonse and M. Hart, Z. Physik 188, 154 (1965).
[7]S. Tanemura and N. Kato, to be published.

MICROWAVE EMISSION FROM n-TYPE INDIUM ANTIMONIDE AT 4.2 AND 77°K *

G. Bekefi
Department of Physics and Research Laboratory of Electronics,
Massachusetts Institute of Technology, Cambridge, Massachusetts

and

A. Bers and S. R. J. Brueck
Department of Electrical Engineering and Research Laboratory of Electronics,
Massachusetts Institute of Technology, Cambridge, Massachusetts

(Received 10 April 1967)

Indium antimonide emits microwave noise when it is subjected simultaneously to parallel dc electric and magnetic fields whose values exceed certain thresholds. Comparison of the emission characteristics at 77°K with those at 4.2°K shows two major differences: (a) The threshold magnetic field at 4.2°K is approximately half that at 77°K. (b) With increasing magnetic field the emission at 4.2°K is comprised of a background continuum upon which are superposed equally spaced resonant spikes; at 77°K the background continuum only is observed.

Larrabee[1] and Hicinbothem[2] were the first to observe microwave emission from n-type InSb when a sample was subjected simultaneously to dc magnetic and electric fields. The threshold values of B_0 and E_0 for onset of the emission were approximately 3000 G and 200 V/cm, respectively. At these high electric fields, electron-hole avalanche occurs, and Steele[3] attributes the microwave emission to photoconductive mixing of band-gap radiation.

Buchsbaum, Chynoweth, and Feldmann,[4] and others,[5-7] have found another regime of microwave emission at relatively low electric fields ($E_0 \approx 10$ V/cm), well below values of E_0 required for avalanche breakdown, where the sample exhibits nearly linear current-voltage characteristics. This report is concerned exclusively with this low-field regime.

It has been suggested[8,9] that the instability arises from phonons that are excited by the drifting electrons. The unstable longitudinal wave then couples to an electromagnetic wave at the boundary of the sample. If this is indeed the mechanism, the phonon lifetime plays a

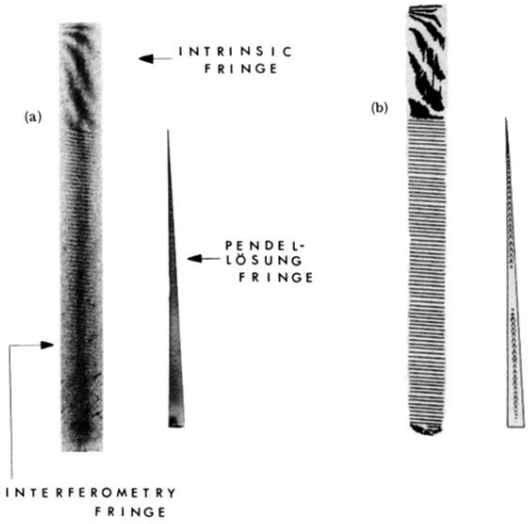

FIG. 2. Photograph (a) and schematic illustration (b) of the three kinds of fringes. The tip of the Pendellösung fringes corresponds to the boundary between the intrinsic fringes and the interferometry fringes. If the specimen crystal is absent, the intrinsic fringes cover the region of the interferometry fringes.